

# Magnetostatic energies of spherical particles

R. CAREY

Department of Applied Physics, Lanchester Polytechnic, Coventry

*MS. received 21st May 1971*

**Abstract.** The demagnetizing energy or magnetostatic self energy of a spherical particle is calculated for two groups of magnetic 'free pole' configuration. The groups are chosen so that the calculated energies are directly applicable to problems concerning (a) non-magnetic inclusions in uniaxially magnetized domains and supporting 'spikes' of reverse magnetization and (b) spherical magnetic particles of uniaxial materials containing few domains. The results are presented in graphical form but the various equations should be easily applied to different problems.

## 1. Introduction

In any calculation of the energy of a domain structure where magnetic 'free pole' effects are present, the estimation of the demagnetizing or magnetostatic self energy of the system is always a primary problem.

Problems concerning the domain structures associated with spherical or near-spherical particles arise in connection with magnetic materials in two separate fields of study. Firstly, they occur in the study of the effects of non-magnetic inclusions on the general properties of magnetic materials. In such cases the shape and size of the closure domain structures that form at the inclusions and the interaction between inclusions and moving domain boundaries are both matters that strongly influence the nature of the magnetization reversal process. Such effects relate directly to the nucleation and coercive fields of the material. The second field of interest is in the study of fine magnetic particles, when the sizes of the particles to be considered are just greater than the upper limit of the single domain region, so that the particles now contain a few domains. In both of these areas a knowledge of the magnetostatic energy of the particular domain configuration associated with the particles is essential for a full study and analysis of the possible magnetic states. Similar calculations of magnetostatic energies have been performed for uniformly magnetized rectangular blocks (Rhodes and Rowlands 1954).

The calculations presented here refer only to spherical particles with associated domain boundaries that are assumed to be of negligible thickness, so that the energies obtained are only adequate approximations for particles which may be considered large relative to the boundary width in the material being considered.

## 2. Method

In general, the magnetic potential of a magnetized body is related to the 'effective' surface and volume charges or 'free poles' and may be written

$$V = V_s + V_v = \int \frac{\sigma_s \, d\sigma}{r} + \int \frac{\sigma_v \, d\tau}{r}. \quad (1)$$

In the systems about to be considered the magnetization of the body is assumed to be uniform throughout the volume of the material, so that  $\text{div } \mathbf{M} = 0$  and the only contribution to the final potential is that due to the 'equivalent surface magnetic charge'. Thus the calculation of the magnetostatic self energy becomes equivalent to the calculation of the

electrostatic energy for a given surface-charge distribution. The required potential is that which satisfies Laplace's equation  $\nabla^2 V_s = 0$ .

In each case a particular surface-charge density is first expanded as a series of Legendre polynomials. The potentials  $V_i$  and  $V_e$  at internal and external points respectively of the particle are obtained by superposition and used in the relation

$$\left(\frac{\partial V_e}{\partial r} - \frac{\partial V_i}{\partial r}\right)_{r=R} = 4\pi\sigma_s \tag{2}$$

to obtain the potential at the surface. Finally, the magnetostatic energy is calculated as

$$E_m = \frac{1}{2} \int \sigma_s V_s \, ds \tag{3}$$

the integral being taken over the particle surface.

In all cases the resulting equation for the magnetostatic energy is in the form of a convergent series. The summation of each series has been performed with the aid of a computer and has been continued until successive terms differed by less than  $10^{-5}$ , a condition which usually required the summation of at least thirty terms.

Case 1

In the first system the charge distribution refers directly to two real domain phenomena in magnetic materials. The particular arrangement is shown in figure 1, where it can be seen that the distribution of surface charge is identical for (a) a spherical non-magnetic

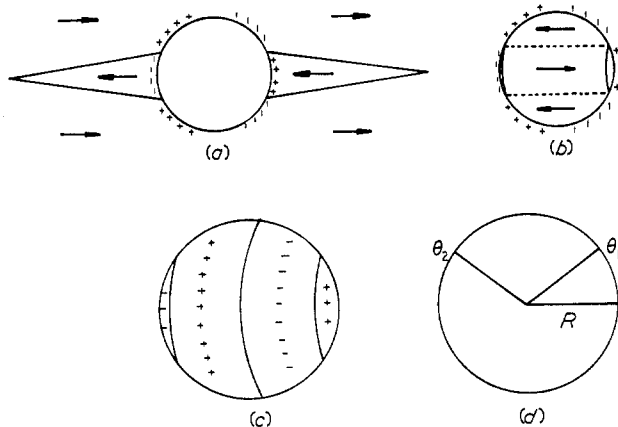


Figure 1. Surface 'free poles' due to (a) two spikes of reverse magnetization at a non-magnetic inclusion and (b) a cylindrical domain boundary within a spherical magnetic particle. The subdivision of the surface charge is shown in (c) with the coordinates in (d).

inclusion supporting nucleated 'spikes' of reverse magnetization and (b) a spherical magnetic particle divided into domains by a cylindrical domain boundary. In (a) the calculation refers only to the 'free pole' distribution at the surface of the inclusion: the energy associated with the 'free poles' at the surfaces of the reverse spike domains is not included.

The detailed steps in the calculation are given in appendix 1. The magnetostatic energy of the system shown in figure 1(c) is

$$E_m = 8\pi^2 M_s^2 R^3 \left\{ \left(\frac{\beta^2 - \alpha^2}{2} - \frac{\alpha^2}{2}\right) + \left(\frac{1 + \beta^3 - \alpha^3}{9}\right) + \sum_{n=2}^{\infty} \left(\frac{a_n}{2n+1}\right)^2 \right\} \tag{4}$$

where  $\alpha = \cos \theta_1$ ,  $\beta = \cos \theta_2$ ,  $\theta_1$  and  $\theta_2$  denote the coordinates of the transition in the magnetization direction at the particle surface and

$$a_n = \beta(P_{n+1}(\beta) - P_{n-1}(\beta)) - \alpha(P_{n+1}(\alpha) - P_{n-1}(\alpha)).$$

For the particular case of two identical reverse spikes or a single cylindrical domain boundary, that is when  $\beta = -\alpha$ , this equation reduces to

$$E_m = 8\pi^2 M_s^2 R^3 \left\{ \frac{(1 - 2\alpha^3)^2}{9} + \alpha^2 \sum_{n=2}^{\infty} \left( \frac{\{1 + (-1)^{n+1}\} (P_{n-1}(\alpha) - P_{n+1}(\alpha))}{2n+1} \right)^2 \right\}. \quad (5)$$

Energies computed from (4) are plotted against  $\alpha$  in figure 2, with  $\beta$  as a parameter for the range  $-1 < \beta < 0 < \alpha < 1$ . These curves strictly only apply to a non-magnetic inclusion supporting two reverse spikes of different base diameters. Although this state is not entirely ruled out, a structure of two identical spikes is more commonly observed, in which case the energy is given by (5), and this is plotted as a function of  $\alpha$  ( $= -\beta$ ) in figure 3. (The energy of the single spike configuration is plotted for comparison.)

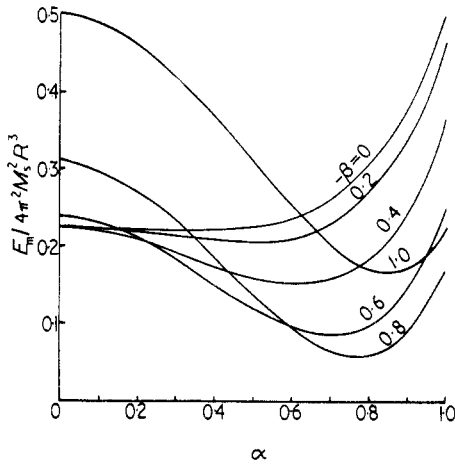


Figure 2. Reduced magnetostatic energies for the system shown in figure 1 plotted against  $\alpha = \cos \theta_1$  with  $\beta = \cos \theta_2$  as a parameter.

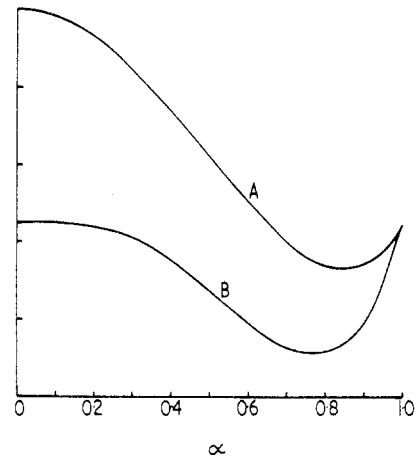


Figure 3. Reduced magnetostatic energies plotted against  $\alpha = \cos \theta_1$  for the special cases where  $\beta = -1$  (curve A), equivalent to the case of a single reverse spike, and  $\beta = -\alpha$  (curve B), equivalent to two identical spikes or a single cylindrical boundary.

Case 2

In this system the charge distribution refers to the spherical particle subdivided by one or more plane boundaries. The boundaries may be either plane domain walls in the magnetic material surrounding a non-magnetic inclusion or plane domain walls within a spherical magnetic particle. The case of the particle divided by a single boundary has been dealt with previously by Néel (1944), when he considered the effects of inclusions on the coercivity. His calculation is repeated and extended to include further subdivisions

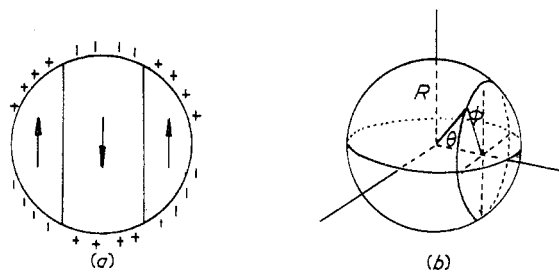


Figure 4. (a) Surface 'free poles' when a particle is subdivided by plane boundaries; (b) shows the coordinate system.

by plane boundaries. Figure 4 shows the charge distribution and the coordinates of the system. The details of the calculation are given in appendix 2.

For the two-boundary state the magnetostatic energy is given by

$$E_m = 4\pi^2 M_s^2 R^3 \left( \frac{2\{1 + \beta(3 - \beta^2)/2 - \alpha(3 - \alpha^2)/2\}^2}{9} + \sum_{n=2}^{\infty} \frac{n(n+1)}{(2n+1)^2} c_n^2 \right) \quad (6)$$

where  $\alpha = \cos \theta_1$ ,  $\beta = \cos \theta_2$  and

$$c_n = \frac{P_n(\beta) - P_{n-2}(\beta)}{2n-1} - \frac{P_{n+2}(\beta) - P_n(\beta)}{2n+3} - \frac{P_n(\alpha) - P_{n-2}(\alpha)}{2n-1} + \frac{P_{n+2}(\alpha) - P_n(\alpha)}{2n+3}.$$

For the special situation where the boundaries are symmetrically disposed about the particle centre (6) reduces to

$$E_m = 4\pi^2 M_s^2 R^3 \left[ \frac{2\{1 - \alpha(3 - \alpha^2)\}^2}{9} + \sum_{n=2}^{\infty} \frac{n(n+1)}{(2n+1)^2} \times \left\{ \{(-1)^n - 1\} \left( \frac{P_n(\alpha) - P_{n-2}(\alpha)}{2n-1} - \frac{P_{n+2}(\alpha) - P_n(\alpha)}{2n+3} \right) \right\}^2 \right]. \quad (7)$$

Energies calculated from (6) are plotted against  $\alpha$  in figure 5 with  $\beta$  as a parameter for the range  $-1 < \beta < 0 < \alpha < 1$ . Equation (7) is shown plotted against  $\alpha$  ( $= -\beta$ ) in figure 6 with the single-boundary energies ( $\beta = -1$ , equivalent to the results given by Néel (1944)) for comparison.

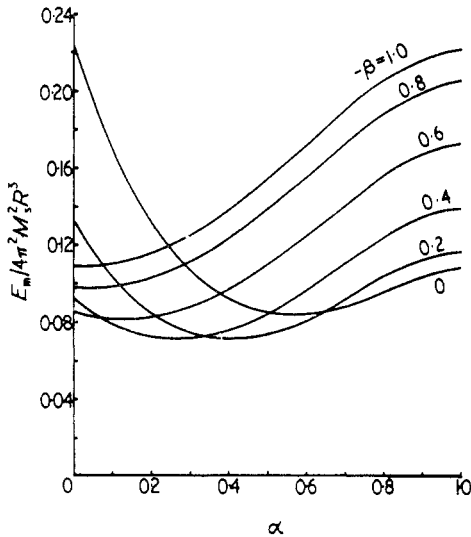


Figure 5. Reduced magnetostatic energies plotted against  $\alpha = \cos \theta_1$  with  $\beta = \cos \theta_2$  as a parameter for the particle with two plane boundaries.

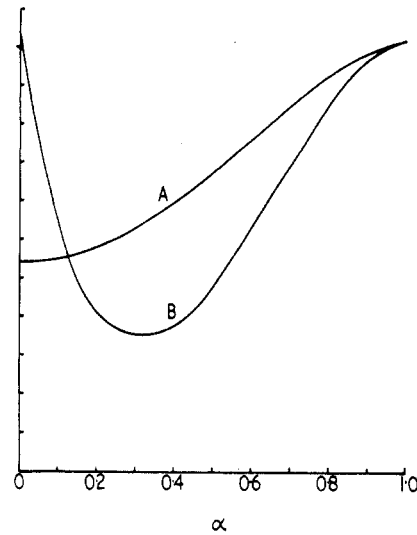


Figure 6. Reduced magnetostatic energies plotted against  $\alpha = \cos \theta_1$  for the special cases of  $\beta = -1$  (curve A), the single boundary, and  $\beta = -\alpha$  (curve B), two boundaries symmetrically disposed about the particle centre.

### 3. Discussion

The magnetostatic energy of an isolated spherical particle, whether non-magnetic within a uniformly magnetized region or a uniformly magnetized single domain, is given by  $\frac{1}{2}NM_s^2$  per unit volume. With  $N=4\pi/3$  for a sphere, this is equal to  $\frac{2}{3}\pi^2 M_s^2 R^3$ , which is in turn given by the value 0.222 in the reduced units used to plot the equations given here (reduced energy =  $E/4\pi^2 M_s^2 R^3$ ). Figure 3 shows how this value is reduced by the nucleation

of a single reverse spike (in the case of the non-magnetic inclusion), reaching 0.162 when  $\alpha=0.86$ , at which point the base diameter of the spike would be approximately equal to  $R$ . Further reduction of the magnetostatic energy is only achieved by the introduction of a further spike, that is by further subdivision of the surface charges. The minimum energy for two identical spikes is 0.057 when  $\alpha=0.76$  and the base diameters of the spikes are approximately  $1.3R$ . This latter value of the magnetostatic energy is considerably less than that of the isolated inclusion and is certainly much lower than a value assumed for this domain configuration in a previous study of reverse spike nucleation at non-magnetic inclusions in uniaxial materials (Carey and Isaac 1964). The values for the two identical spike configuration refer also, of course, to the particle containing a single cylindrical domain boundary.

The energies calculated for the magnetic particle divided by a single plane domain boundary are very slightly different to those already given by Néel (1944). The difference is only apparent at the energy minimum, where the value calculated here is 0.108 compared with a value of 0.102 given by Néel. This is due to the fact that this value is obtained after the summation of about 40 terms whereas Néel's figure was obtained from the first five terms of the series.

With two plane boundaries the magnetostatic energy of most arrangements of the positions of the boundaries is less than that of a particle with a single boundary at its centre, that is less than 0.108. For symmetrical dispositions of the two boundaries the magnetostatic energy reaches a minimum value of 0.071 (see figure 6), when both the boundaries are approximately  $0.3R$  from the centre of the particle.

### Appendix 1

For the configuration shown in figure 1(c) the charge distribution is

$$\sigma_s = \epsilon M_s \cos \theta, \quad \epsilon = \begin{cases} 1 & \text{for } 0 < \theta < \theta_1 \\ -1 & \text{for } \theta_1 < \theta < \theta_2 \\ 1 & \text{for } \theta_2 < \theta < \pi \end{cases}$$

which is expanded as

$$\sigma_s(\mu) = a_0 P_0(\mu) + a_1 P_1(\mu) + \dots + a_n P_n(\mu)$$

where  $\mu = \cos \theta$  and  $P_n(\mu)$  is a Legendre polynomial.

Hence

$$a_n = \frac{2n+1}{2} \int_{-1}^1 \sigma_s(\mu) P_n(\mu) d\mu$$

so that

$$\sigma_s(\mu) = M_s \left\{ \left( \frac{\beta^2}{2} - \frac{\alpha^2}{2} \right) - \mu(1 + \beta^3 - \alpha^3) + \sum_{n=2}^{\infty} a_n P_n(\mu) \right\}$$

where

$$a_n = \beta(P_{n+1}(\beta) - P_{n-1}(\beta)) - \alpha(P_{n+1}(\alpha) - P_{n-1}(\alpha))$$

$\alpha = \cos \theta_1$  and  $\beta = \cos \theta_2$ .

The potentials are, therefore,

$$V_e = 4\pi R M_s \left\{ \left( \frac{\beta^2}{2} - \frac{\alpha^2}{2} \right) \frac{R}{r} + \frac{(1 + \beta^3 - \alpha^3)}{3} \left( \frac{R}{r} \right)^2 \mu + \sum_{n=2}^{\infty} \frac{a_n}{2n+1} \left( \frac{R}{r} \right)^{n+1} P_n(\mu) \right\}$$

and

$$V_i = 4\pi R M_s \left\{ \left( \frac{\beta^2}{2} - \frac{\alpha^2}{2} \right) + \frac{(1 + \beta^3 - \alpha^3)}{3} \left( \frac{r}{R} \right) + \sum_{n=2}^{\infty} \frac{a_n}{2n+1} \left( \frac{r}{R} \right)^n P_n(\mu) \right\}$$

which with equations (3) and (4) lead to (5).

**Appendix 2**

The charge distribution is now shown in figure 4(a) and is given by

$$\sigma_s = \epsilon M_s \sin \theta \cos \phi, \quad \epsilon = \begin{cases} 1 & \text{for } 0 < \theta < \theta_1 \\ -1 & \text{for } \theta_1 < \theta < \theta_2 \\ 1 & \text{for } \theta_2 < \theta < \pi \end{cases}$$

which is expanded in the form

$$\sigma_s(\mu) = (c_1 P_1'(\mu) + c_2 P_2'(\mu) + \dots + c_n P_n'(\mu)) \sin \theta \cos \phi.$$

Hence

$$\int_{-1}^1 (1 - \mu^2) P_n'(\mu) P_m'(\mu) d\mu = \begin{cases} 0 & \text{for } n \neq m \\ \frac{2n(n+1)}{2n+1} & \text{for } n = m \end{cases}$$

so that

$$c_n = \frac{P_n(\beta) - P_{n-2}(\beta)}{2n-1} - \frac{P_{n+2}(\beta) - P_n(\beta)}{2n+3} - \frac{P_n(\alpha) - P_{n-2}(\alpha)}{2n-1} + \frac{P_{n+2}(\alpha) - P_n(\alpha)}{2n+3}.$$

The potentials are now

$$V_e = \left( a_1 \frac{P_1'}{r^2} + \dots + a_n \frac{P_n'}{r^{n+1}} \right) \sin \theta \cos \phi$$

and

$$V_i = (b_1 P_1' r + \dots + b_n P_n' r^n) \sin \theta \cos \phi$$

and using equation (3) we have

$$\frac{a_n}{R^{n+1}} = b_n R^n; \quad 4\pi M_s c_n = (n+1) \frac{a_n}{R^{n+2}} + n b_n R^{n-1}$$

to give the potential at the surface. Substitution into (4) leads to equation (6) for the energy.

**Acknowledgment**

The author would like to express his thanks to the Science Research Council for financial support.

**References**

CAREY, R., and ISAAC, E. D., 1964, *Br. J. appl. Phys.*, **15**, 551-4.  
 NÉEL, L., 1944, *Cah. Phys.*, **25**, 21-44.  
 RHODES, P., and ROWLANDS, G., 1954, *Proc. Leeds Phil. Soc.*, **6**, 191-210.